Evolution Law of Porosity and Permeability in In-Situ Pyrolysis Zone of Oil Shale

Yunfeng Zhang[1,2], Pengfei Jiang[3], Changsuo Li[1,2], Zhiqiang Zhao[1,2*], Shuai Gao[1,2], Song Yao[1,2], Haibo Sui[1,2], Jiaqi Huang[3]

[1] 801 Institute of Hydrogeology and Engineering Geology, Shandong Provincial Bureau of Geology & Mineral Resources, Jinan 250014, China
[2] Shandong Engineering Research Center for Environmental Protection and Remediation on Groundwater, Jinan 250014, China
[3] College of Geology and Environment, Xi'an University of Science and Technology, Xi'an 710054, China

Corresponding Author Email: zzq0912@163.com

ABSTRACT

This paper tested the permeability and porosity of oil shale during the pyrolysis process. Combined with the in-situ pyrolysis simulation, this paper analyzed and discussed the evolution of permeability and porosity in the oil shale in-situ pyrolysis zone through electric heating technology. During the pyrolysis of oil shale, the porosity and permeability increased significantly when temperature ranged from 300℃ to 500℃. The scope of the in-situ pyrolysis zone expanded with the increase of heating time and pyrolysis saturation was reached essentially after six years of heating. After in-situ pyrolysis, oil shale's permeability and porosity changed greatly within 7.5 meters in the vertical direction and 4.8 meters in the horizontal direction from the central wellbore of the heating well. Oil shale in this area changed from aquifuge to aquitard.

1. INTRODUCTION

Oil shale is a sedimentary rock with high ash contents and combustible organic matters. Shale oil and combustible gas can be obtained through dry distillation, and shale oil processed into a variety of refined oil [1-3]. China is a big energy consumer, but its conventional energy supply is still grim [4]. As a typical unconventional oil and gas resource, the reserves of oil shale are huge. According to statistics, oil shale reserves in China are 1.005 trillion tons, equivalent to 570 billion tons of shale oil reserves. Oil shale has broad development and utilization prospects [5, 6].

There are two main development technologies for oil shale: the ground retorting technology and the underground in-situ pyrolysis technology. At present, China mainly adopts the first technology to develop and utilize the oil shale. But this technology requires shallowly buried oil shale layers, high oil content and harsh mining conditions, and the "three wastes" (wastewater, waste gases and residues) caused by this mining technology are also paid much attention. For the second mining technology, shale oil and gas are produced only by heating the oil shale in the original stratum [7-9]. Compared with the ground retorting technology, this technology reduces the cost of excavation and transportation, effectively avoids the environmental pollution caused by the former, and does not need to destroy the oil shale layer, showing advantages in safety, environmental protection and high economic benefits.

Oil shale is a dense rock, with low permeability under natural conditions and poor thermal conductivity. After pyrolysis at high temperature, oil and gas are produced. After pyrolysis, the oil shale generates a lot of pores, where the oil and gas products migrate, leading to changes in the permeability of the oil shale layer [10, 11]. After in-situ pyrolysis, oil shale changes from a dense state to a porous state.

The changes in permeability and porosity may lead to the transformation of oil shale from aquifuge to aquitard, which may affect the flow field of groundwater when the underground hydrogeological conditions change. Many researchers have investigated the mechanism of permeability evolution during oil shale pyrolysis. Wang et al. [12] tested and studied the permeability and the porosity of oil shale samples after steam pyrolysis through the steady-state method, and compared it with the direct retorting process. The results showed that the increase in permeability of oil shale in the parallel bedding direction after high temperature steam pyrolysis was significantly higher than that of the direct retorting mode. Yang et al. [13] studied the influence of pyrolysis temperature on the microstructure of oil shale through a high resolution micro-CT experiment system. The results showed that oil shale changed from a dense and low-permeability rock to a porous and high-permeability medium gradually during the heating process. When the pyrolysis temperature reached 600℃, a lot of pores in oil shale were connected. Zhao and Kang [14] studied the permeability evolution of oil shale in in-situ pyrolysis conditions through the high temperature triaxial permeability experimental system, showing the good correlation between the porosity and permeability evolution of oil shale. With the increase in temperature, oil shale evolved from its original dense state to a porous medium with developed pores, and its porosity and permeability increased. Burnham [15] established a mathematical model of porosity and permeability of the Green River oil shale during retorting, and calculated the modified Kozeny-Carman relationship between permeability and oil shale grade and fraction. Wang et al. [16] studied the macroscopic permeability characteristics of oil shale with temperature and pore pressure by using a high-temperature triaxial permeability test bench. The results showed that the

permeability of oil shale changed slightly between 200-350℃, and increased greatly between 350-550℃. However, the permeability growth rate slowed down between 550-650℃. With the increase in pore pressure, the permeability decreased rapidly and then slowly.

This paper tested the porosity and permeability of oil shale samples at different pyrolysis temperatures through gas measurement. Combined with the simulated temperature field of oil shale in in-situ pyrolysis, this paper analyzed and discussed the evolution of porosity and permeability of the oil shale in in-situ pyrolysis zone in the electric heating in-situ pyrolysis process. The results provided a theoretical basis for the evaluation of formation characteristics after oil shale in-situ pyrolysis.

2. SAMPLES AND EXPERIMENT

2.1 Samples

The experimental samples were taken from the Fushun open-pit mine. The oil shale samples were collected on site and sealed with wax sealing method in time to prevent weathering and metamorphism. The basic physical parameters of the samples were shown in Table 1.

Table 1. Basic physical parameters of oil shale

	Proximate analysis (wt%)				Ultimate analysis (wt%)			
	Moisture	Ash	Volatile	Fixed carbon	N	C	H	O
Oil shale	4.68	75.91	17.54	1.87	1.91	15.44	2.67	6.62

2.2 Thermogravimetric experiment

For the samples used in the experiment, they were first ground by a coal mill, and then ground with an agate mortar into oil shale particles, less than 0.2 mm in size and about 5 mg in weight. Oil shale thermogravimetric analysis was made by a Netzsch STA 449C thermal analyzer (Germany), with test temperature between 30-750℃. High-purity nitrogen protection was introduced during the experiment, with 10℃/min heating rate and 40 mL/min gas flow rate. The experimental data was automatically collected by the computer.

2.3 Porosity and permeability experiments of oil shale at various pyrolysis temperatures

The massive oil shale samples were heated to 200℃, 300℃, 400℃, 500℃ and 600℃ in a nitrogen atmosphere at 2℃/min heating rate, and then taken out after natural cooling. The normal temperature samples and the five heated samples were processed in a standard cylinder with 25 mm diameter and 50 mm height, respectively. The samples were used for porosity and permeability testing through the QTS-2 gas permeability measuring instrument, with nitrogen as the test gas. With 0.6 Mpa as the original pressure, the porosity and permeability were determined according to the principle of Boyle's law and Darcy's law, respectively. The sample's confining pressure was set to 1 Mpa during the test.

3. NUMERICAL SIMULATION

3.1 Mathematical model

At present, in-situ pyrolysis technology for oil shale is divided into three categories: conduction heating (electric heating), convection heating, and radiation heating. Conduction heating of oil shale is simple to operate, and the technology is relatively mature, but the cost is relatively high [17, 18]. For this technology, the oil shale layer above ground is drilled and then an electric heater is put in the well for heating the oil shale. When heated to the pyrolysis temperature, the kerogen in oil shale is decomposed into gas and shale oil products [19, 20].

As long as there is a temperature difference, heat conduction occurs because it is related to the movement of molecules and atoms in oil shale. Heat conduction follows the heat conduction equation and initial and boundary conditions.

The heat conduction equation is:

$$\lambda \nabla^2 T = \rho c + Q(x, y, z) \tag{1}$$

The initial conditions are:

$$T(x, y, z, 0) = T_0(x, y, z) \tag{2}$$

The boundary conditions are:

$$T\big|_{\Gamma 1} = T_W(x, y, z, t) \; \Gamma \in \Gamma 1 \tag{3}$$

$$\lambda \frac{\partial T}{\partial n}\bigg|_{\Gamma 2} = q(x, y, z, t) \; \Gamma \in \Gamma 2 \tag{4}$$

$$\lambda \frac{\partial T}{\partial n}\bigg|_{\Gamma 3} = h(T_2 - T) \; \Gamma \in \Gamma 3 \tag{5}$$

where, T is the temperature of oil shale formation; t is time; λ is the coefficient of heat conduction for oil shale; c is the specific heat conductivity of oil shale; Q is the source sink term; T_0 is the initial temperature of oil shale; T_w is the wall temperature; T_2 is the fluid temperature on the boundary; q is the fluid density on the boundary; h is the heat transfer coefficient of the boundary; Γ is all the boundary conditions of the control body.

3.2 Numerical simulation model

The geometric model was established by using DM modeling in ANSYS. Both the length and width of the model was 100 m. The thickness of the middle oil shale layer was 20 m. The upper and lower layers in oil shale were mudstone, and the thickness was 30 m. Based on this formation condition, four heating wells were set up, with a diameter of 1 m. The locations of the wells are shown in Figure 1. Then the grid division module Workbench Meshing was used to mesh the geometric model. Figure 2 shows the result.

The simulation parameters were set as follows: the length of the electric heater, which was set in the middle of the oil shale layer, was 10 m; the set temperature was 1000°C, the initial temperature of the formation was 25°C, the oil shale density was 1950 kg/m³, the specific heat capacity was 1000 J/(kg·K), as well as the thermal conductivity was 1.43 W/(m·k). The density of mudstone was 1850 kg/m³, the thermal conductivity was 2.3 W/(m·k), and the specific heat capacity was 880 J/(kg·K).
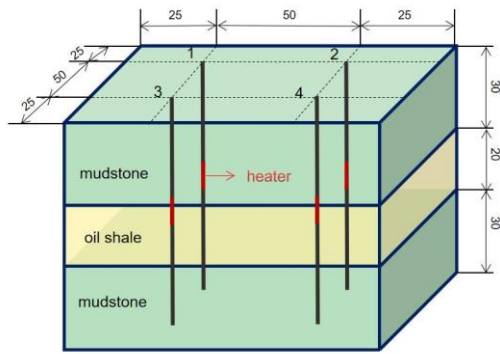

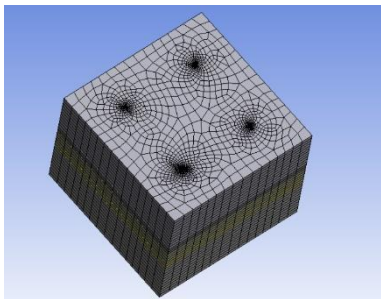**Figure 1.** Numerical simulation model for oil shale in-situ pyrolysis (m)

Figure 2. Grid division of oil shale in-situ pyrolysis model

4. RESULT AND DISCUSSION

4.1 Analysis of thermogravimetric test results

The pyrolysis characteristics of Fushun oil shale were analyzed through thermogravimetric analysis. Figure 3 is the TG/DTG curve, which describes the mass loss of oil shale with an increase in temperature. According to the experimental data, the pyrolysis of oil shale was mainly divided into the following three stages.

The mass loss first mainly occurred at about 100°C. This was oil shale's dehydration stage, involving pore water evaporation in oil shale and removal of some layer water and structural water. With temperature increase, the kerogen in oil shale began to soften, and the small organic molecules began to volatilize. This mainly occurred in the initial heating stage, whose temperature was less than 300°C.

The second stage was the pyrolysis stage for oil shale. As the temperature increased, the kerogen macromolecules in oil shale decomposed and shale oil and gas were generated. For this stage, the total mass loss was 26.2%, with temperature between 300-600°C; the mass loss was 24.6%, with temperature between 350-500°C; the largest mass loss rate occurred at about 460°C.

The third stage mainly involved the pyrolysis of carbonate, clay, and other substances in oil shale. With the increase in temperature, these substances decomposed into CO_2 and absorbed a lot of heat. The mass loss mainly occurred above 600°C.
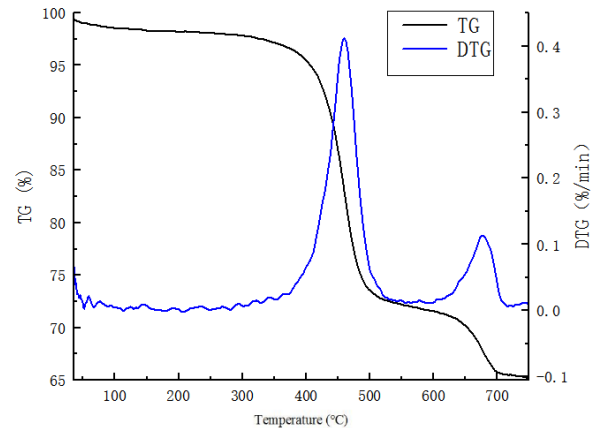

Figure 3. TG and DTG curves of oil shale

Note: TG and DTG stand for thermogravimetry and differential thermogravimetry, respectively.

4.2 Analysis of porosity and permeability test of oil shale

Many factors affected the porosity and permeability of oil shale during pyrolysis. For example, pyrolysis of organic matter, connectivity or blockage of pore channels arising from thermal cracking of the mineral skeleton, and changes in the physical properties of oil shale during pyrolysis all contributed to mineral degradation. These factors affected the variation of oil shale permeability, and the permeability varied in different temperature ranges. As shown in Figure 4, the change of permeability and porosity of oil shale with temperature can be divided into the following stages.
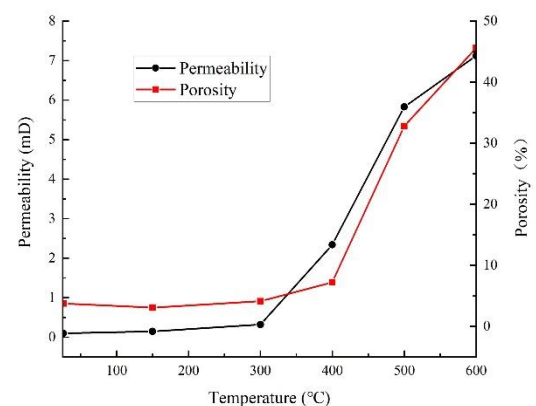

Figure 4. Curves of permeability and porosity of oil shale with pyrolysis temperature

In the first stage with temperature ranging from room temperature to 300°C, the porosity of oil shale changed weakly, the permeability was extremely low and changed little with temperature. The organic matters had not yet reached the pyrolysis temperature, but some free water inside the oil shale evaporated, the kerogen began to soften, and some gas escaped.

The oil shale expanded and deformed, and thermal stress was generated between the inorganic mineral particles consisting of the mineral skeleton, resulting in the formation of small pores and cracks inside the oil shale. Permeability of the oil shale changed from 0.1 mD to 0.32 mD, and the porosity changed from 3.76% to 4.13%.

In the second stage with temperature ranging from 300℃ to 500℃, the porosity continued to grow, and the increase was obviously larger. At the same time, the permeability and porosity increased synchronously. This was the main stage of permeability change in oil shale, caused mainly by the pyrolysis of oil shale. Organic matters in the oil shale gradually began to pyrolyze, gradually forming shale oil and gas. As these products began to break away from the mineral skeleton, the pores increased accordingly. In addition, the escape of the product had a certain pore expansion effect, causing the oil shale to form a larger seepage channel. The permeability increased from 0.32 mD to 5.83 mD, and the porosity increased from 4.13% to 32.78%.

In the third stage with temperature ranging from 500℃ to 600℃, the porosity and permeability still showed an increasing trend, but the increase was slightly smaller than that in the previous temperature range. At this stage, organic matters basically completed the pyrolysis reaction, and the escape of pyrolysis products had a certain pore expansion impact on oil shale pores. In addition, the uneven thermal stress arising from the asynchronous thermal expansion of inorganic mineral particles led to new seepage channels in oil shale, therefore, the permeability continued to increase.

However, due to the increase of pore fissures, the strength of the mineral skeleton in oil shale decreased and some pores and fractures collapsed and blocked, thus inhibiting the increase of permeability. The permeability increased from 5.83 mD to 7.12 mD, and the porosity increased from 32.7 % to 45.6 %, which was smaller than that in the previous stage.

4.3 Temperature field of oil shale during in-situ pyrolysis

Transient simulation was carried out based on the model, with the heating simulated for nine years. Two sections were intercepted to show the evolution law of the temperature field. Figure 5 shows the specific section positions.

Figure 6 shows the temperature field of different heating time in the longitudinal section of the oil shale layer connected by well 1 and well 2. Figure 7 is the temperature field of different heating time in the transverse section in the middle of the oil shale layer. The temperature diffusion range and effective heating volume of oil shale gradually increased as heating time increased. On the horizontal section, the temperature diffused mainly in a circular shape centered on the heating well, while the temperature diffused around in an approximate water bottle shape on the vertical section. According to Figure 6 and Figure 7, when the oil shale was heated for one month, the high temperature range was very small, with only a small part of the oil shale near the heating well reaching the pyrolysis temperature (300-500℃). The pyrolysis range obviously expanded as heating time increased.
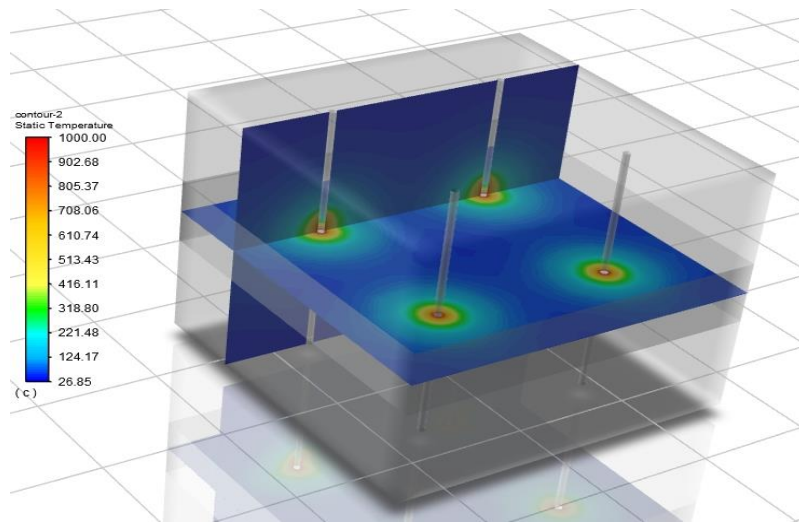

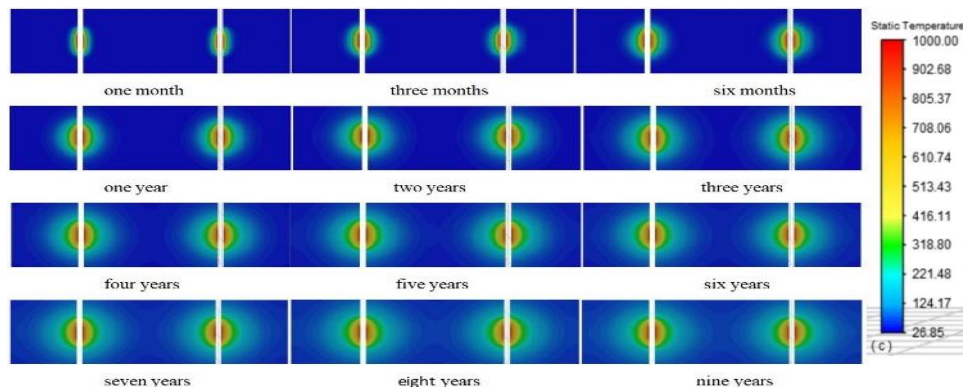**Figure 5.** Horizontal and vertical section positions of the simulation

Figure 6. Temperature field of oil shale during pyrolysis in vertical section
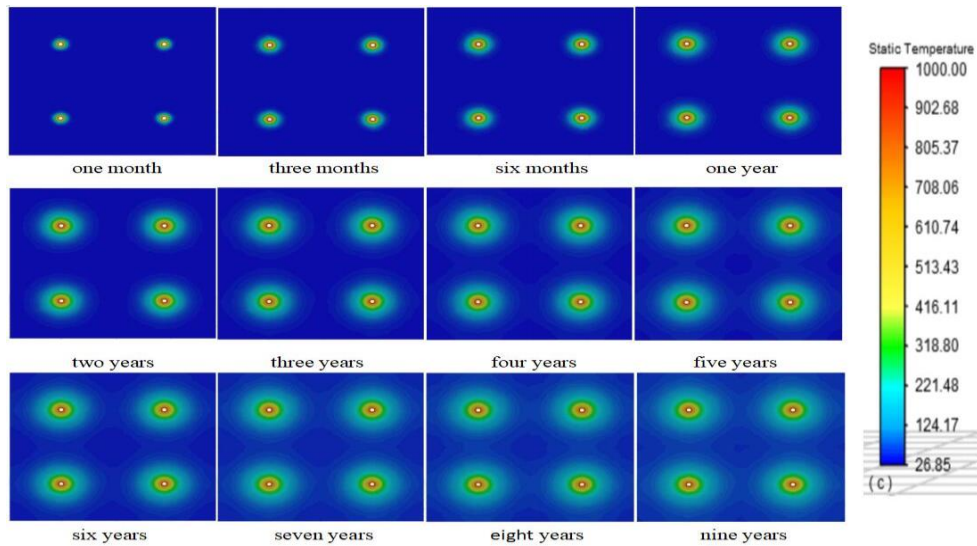
Figure 7. Temperature field of oil shale during pyrolysis in horizontal section

When heating of the oil shale continued till the 6th year, the pyrolysis range no longer significantly changed, and the pyrolysis saturation state was basically reached. The effective heating volume of oil shale was about 7608.32 m³. From the 6th to the 9th year of heating, the temperature of the oil shale layer rose slowly, and the effective heating volume was about 8490.56 m³. With the increase in heating time, the temperature of the oil shale layer close to the heating well increased quickly, which was close to the temperature of the well wall. At this time, the heat transfer between the heating well and the oil shale layer obviously reduced. After six years of heating, the temperature of the oil shale layer did not change significantly, and the subsequent heating was meaningless. Therefore, the simulation only considered six-year heating.

4.4 Evolution law of porosity and permeability of oil shale in-situ pyrolysis

Combined with oil shale thermogravimetric analysis, the results of the gas permeability experiment, and the temperature field distribution obtained by oil shale in-situ pyrolysis simulation, the permeability and porosity variation curves of different regions after in-situ pyrolysis of oil shale were obtained. Due to the symmetrical arrangement of heating wells in the model, only well 1 was selected for analysis. With the center of the heating well wall as the starting point, the research scope included 10 m to the top of the oil shale layer on the vertical dimension, and 24.5 m to the left boundary of the oil shale layer on the horizontal dimension.

In the vertical direction, Figure 8 shows the temperature increase of oil shale along with time. The farther away from the borehole wall, the lower the temperature of the oil shale. The oil shale could not reach the pyrolysis temperature (300-500°C) about 7.5 m away from the well-wall center. Figure 9 and Figure 10 show that the permeability and porosity of oil shale increase with heating time. The farther away from the wellbore, the lower the permeability and porosity of oil shale. When the oil shale was heated for 6 years，within the range of about 7.5 m from the center of the wellbore, the temperature of the oil shale layer changed greatly, leading to great changes in the permeability and porosity. However, the permeability and porosity changed little beyond about 7.5 m from the wellbore center.
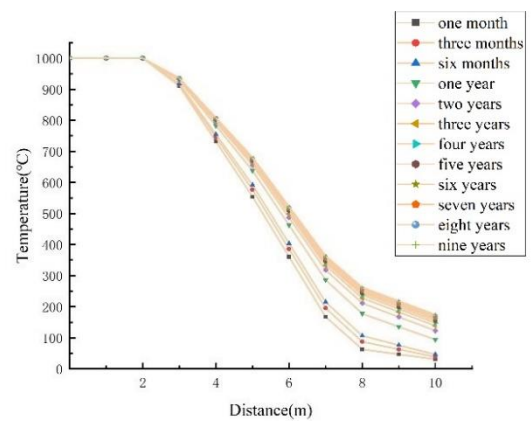

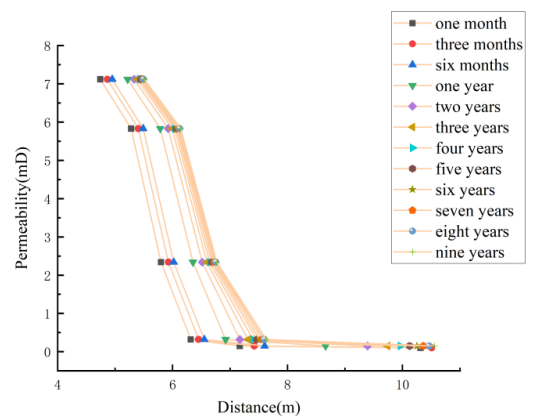**Figure 8.** Curves of temperature with distance in longitudinal section at different heating time

Figure 9. Curves of permeability with distance in longitudinal section at different heating time

In the horizontal direction, Figure 11 shows that the gradual temperature increase of oil shale along with the increase in heating time, and the change in temperature is higher than that in the vertical direction. The farther away from the wellbore center, the lower the oil shale temperature. The oil shale could not reach the pyrolysis temperature about 4.8 m away from the center of the wellbore. Figure 12 and Figure 13 show that the

permeability and porosity of the oil shale layer increase with heating time. The farther away from the wellbore center, the lower the permeability and porosity of oil shale. When the oil shale was heated for 6 years，within the range of about 4.8 m from the wellbore center, the temperature of the oil shale layer changed greatly, and the permeability and porosity also changed greatly. The permeability and porosity changed little beyond about 4.8 m from the center of the wellbore.
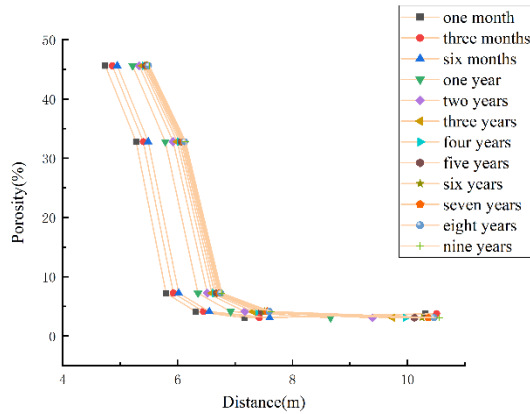

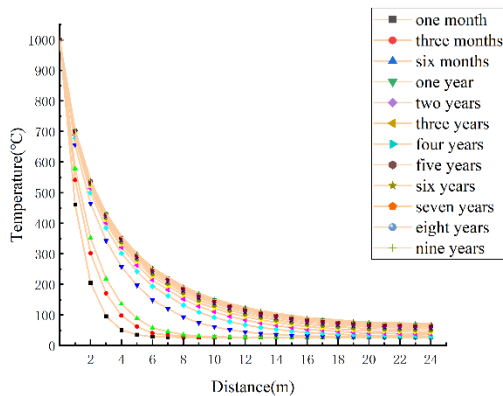**Figure 10.** Curves of porosity with distance in longitudinal section at different heating time

Figure 11. Curves of temperature with distance in transverse section at different heating time
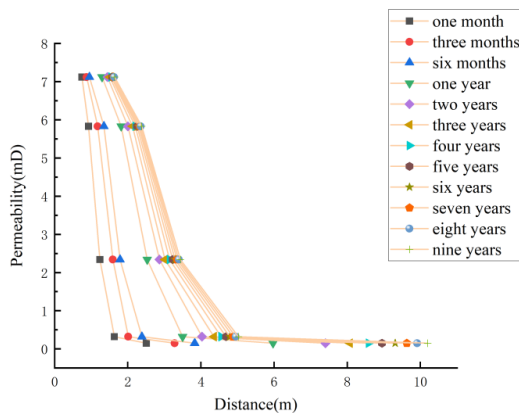

Figure 12. Curves of permeability with distance in transverse section at different heating time
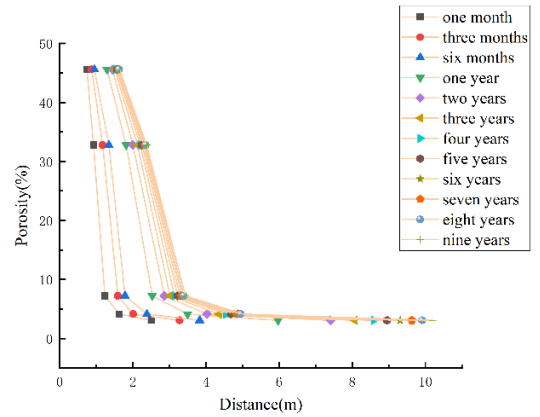

Figure 13. Curves of porosity with distance in transverse section at different heating time

5. CONCLUSIONS

(1) When oil shale's heating temperature was lower than 300°C, the porosity and permeability changed little. The porosity increased to 32.78% and the permeability increased to 5.83 mD when temperature ranged from 300°C to 500°C. The increase was obvious mainly because of the pyrolysis of organic matters. With temperature higher than 500°C, the porosity and permeability of oil shale continued to increase, but the increase slowed down.

(2) In the process of electric heating for in-situ pyrolysis of oil shale, the heat was transferred to the oil shale from the heating well. When the heating time was six years, the effective pyrolysis zone had a basically stable scope and the pyrolysis saturation state was reached.

(3) After six years of heating, the permeability and porosity in the in-situ pyrolysis zone changed greatly within 7.5 m from the center of the heating well in the vertical direction and within 4.8 m from the center in the horizontal direction.

ACKNOWLEDGMENT

REFERENCES

[1] Dyni, J.R. (2006). Geology and resources of some world oil-shale deposits. Oil Shale, 20(3): 193-252.

[2] Bansal, V.R., Kumar, R., Sastry, M.I.S., Badhe, R.M., Kapur, G.S., Saxena, D. (2019). Direct estimation of shale oil potential by the structural insight of Indian origin kerogen. Fuel, 241: 410-416. https://doi.org/10.1016/j.fuel.2018.12.057

[3] Niu, M., Wang, S., Han, X., Jiang, X. (2013). Yield and characteristics of shale oil from the retorting of oil shale and fine oil-shale ash mixtures. Applied Energy, 111: 234-239. https://doi.org/10.1016/j.apenergy.2013.04.089

[4] Ni, X., Miao, J., Lv, R., Lin, X. (2017). Quantitative 3D spatial characterization and flow simulation of coal

macropores based on μCT technology. Fuel, 200: 199-207. https://doi.org/10.1016/j.fuel.2017.03.068

[5] Washburn, K.E., Birdwell, J.E., Foster, M., Gutierrez, F. (2015). Detailed description of oil shale organic and mineralogical heterogeneity via Fourier transform infrared microscopy. Energy & Fuels, 29(7): 4264-4271. https://doi.org/10.1021/acs.energyfuels.5b00807

[6] Sun, Y.H., Bai, F.T., Lü, X.S., Li, Q., Liu, Y.M., Guo, M.Y., Liu, B.C. (2015). A novel energy-efficient pyrolysis process: self-pyrolysis of oil shale triggered by topochemical heat in a horizontal fixed bed. Scientific Reports, 5(1): 1-8. https://doi.org/10.1038/srep08290

[7] Li, Q., Wei, H., Zhang, Y., Han, L., Han, S., Ding, N. (2020). The variations on thermal conductivity and structures of silty clay modified by waste fly ash and oil shale ash after freeze–thaw cycles. Construction and Building Materials, 260: 119954. https://doi.org/10.1016/j.conbuildmat.2020.119954

[8] Yang, D., Zhao, Y., Kang, Z. (2019). Numerical simulation of in situ exploitation of oil shale by injecting high-temperature steam. Oil Shale, 36(4): 483-500.

[9] Saif, T., Lin, Q., Singh, K., Bijeljic, B., Blunt, M.J. (2016). Dynamic imaging of oil shale pyrolysis using synchrotron X-ray microtomography. Geophysical Research Letters, 43(13): 6799-6807. https://doi.org/10.1002/2016GL069279

[10] Li, G.Y., Ma, Z.L., Zheng, J.X., Bao, F., Zheng, L.J. (2016). NMR analysis of the physical change of oil shales during in situ pyrolysis at different temperatures. Petroleum Geology & Experiment, 38(3): 402-406. https://doi.org/10.11781/sysydz201603402

[11] Zhao, J., Feng, Z.C., Yang, D., Kang, Z. (2013). Study on distribution characteristics of pores and fissures inside oil shale under the CT experiment. Journal of Liaoning Technical University (Natural Science), 32(8): 1044-1049.

[12] Wang, L., Yang, D., Kang, Z.Q. (2021). Experimental study on permeability characteristics and anisotropy evolution of oil shale after high-temperature water vapor treatment. Chinese Journal of Rock Mechanics and Engineering, 40(11): 2286-2295. https://doi.org/10.13722/j.cnki.jrme.2020.1072

[13] Yang, D., Kang, Z.Q., Zhao, J., Zhao, Y.S. (2011). CT Experiment research of oil shale under high temperature. Journal of Taiyuan University of Technology, 42(3): 255-257.

[14] Zhao, J., Kang, Z.Q. (2021). Permeability of oil shale under in situ conditions: Fushun oil shale (China) experimental case study. Natural Resources Research, 30: 753-763. https://doi.org/10.1007/s11053-020-09717-0

[15] Burnham, A.K. (2018). Thermomechanical properties of the garden gulch member of the green river formation. Fuel, 219: 477-491. https://doi.org/10.1016/j.fuel.2018.01.122

[16] Wang, G., Yang, D., Zhao, Y., Kang, Z., Zhao, J., Huang, X. (2019). Experimental investigation on anisotropic permeability and its relationship with anisotropic thermal cracking of oil shale under high temperature and triaxial stress. Applied Thermal Engineering, 146: 718-725. https://doi.org/10.1016/j.applthermaleng.2018.10.005

[17] Saif, T., Lin, Q., Gao, Y., Al-Khulaifi, Y., Marone, F., Hollis, D., Bijeljic, B. (2019). 4D in situ synchrotron X-ray tomographic microscopy and laser-based heating study of oil shale pyrolysis. Applied Energy, 235: 1468-1475. https://doi.org/10.1016/j.apenergy.2018.11.044

[18] Lin, L., Lai, D., Guo, E., Zhang, C., Xu, G. (2016). Oil shale pyrolysis in indirectly heated fixed bed with metallic plates of heating enhancement. Fuel, 163: 48-55. https://doi.org/10.1016/j.fuel.2015.09.024

[19] Niu, M., Wang, S., Han, X., Jiang, X. (2013). Yield and characteristics of shale oil from the retorting of oil shale and fine oil-shale ash mixtures. Applied Energy, 111: 234-239. https://doi.org/10.1016/j.apenergy.2013.04.089

[20] Bai, F., Sun, Y., Liu, Y., Guo, M. (2017). Evaluation of the porous structure of Huadian oil shale during pyrolysis using multiple approaches. Fuel, 187: 1-8. https://doi.org/10.1016/j.fuel.2016.09.012